

Are Antarctic ozone variations a manifestation of dynamics or chemistry?

Ka-Kit Tung*, Malcolm K. W. Ko†, José M. Rodriguez† & Nien Dak Sze†

* Massachusetts Institute of Technology, Cambridge, Massachusetts 02139, and Clarkson University, Potsdam, New York 13767, USA

† Atmospheric and Environmental Research, Inc., Cambridge, Massachusetts 02139, USA

Observations¹⁻³ reveal a large seasonal decrease in the column density of ozone during Antarctic early spring, followed by a rapid increase after October beyond its pre-spring value. Given the unique circumstances that exist in the Antarctic environment—relatively stable circumpolar vortex, cold air temperature achieved during polar night, and the increase in absorption of solar radiation by ozone as the Sun returns—we surmise the existence of a reverse circulation cell with rising motion in the polar lower stratosphere. The upwelling brings ozone-poor air from below 100 mbar to the stratosphere, possibly contributing to the observed ozone decline in early spring. At the same time, the Antarctic stratosphere might contain a very low concentration (<0.1 p.p.b.v. (parts per 10⁹ by volume) of NO_x(NO+NO₂), a condition that could favour a greatly enhanced catalytic removal of O₃ by halogen species^{2,4,5}. We argue that heterogeneous processes and formation of OCIO by the reaction BrO + ClO → OCIO + Br before and after the polar night might help to suppress the NO_x levels during the early spring period. However, the dilution of the concentrations of the chlorine species by the upwelling may reduce the effectiveness of the photochemical removal of O₃.

The zonal mean transport in the lower stratosphere normally takes the form of a two-cell diabatic circulation, with rising motion in the tropics and subsidence near both poles⁶⁻¹⁰. For a species such as O₃, whose source is in the stratosphere, upward transport tends to reduce its column abundance, as tropospheric air with low O₃ mixing ratio is brought up to the stratosphere. Poleward and downward transport in the subsiding branches tends to increase its abundance at high latitudes. This situation is further accentuated in winter by the downward branch of the one-cell circulation that exists above 25 km (refs 11, 12). The latitudinal distribution of the column abundance of O₃ does not, however, have north-south symmetry^{13,14}, as the spring maximum in the Southern Hemisphere is located closer to the Equator than in the north.

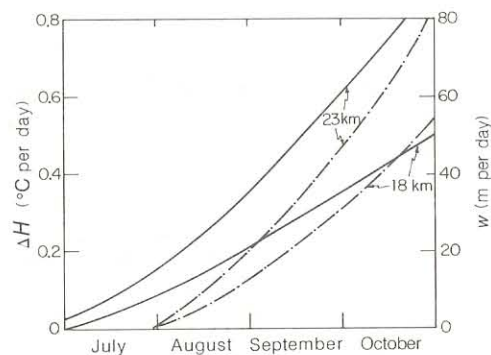


Fig. 1 Calculated heating rate (ΔH) from O₃ absorption over a 24-h period, as a function of time, for 69° S (—) and 76° S (---) at different altitudes. The heating rates are calculated from the local O₃ concentration using the parameterization of Strobel³¹. The time variation mainly reflects the seasonal changes in the number of sunlit hours. The observed O₃ profile from Syowa Station in July is adopted as the initial condition. For this calculation, horizontal transport and photochemical removal are ignored. The O₃ profile is updated in time by accounting for the effect of the upward advection \bar{w} by equation (4). The right-hand scale indicates the approximate value of \bar{w} , assuming that $\Gamma = 10^\circ \text{C km}^{-1}$.

The winter polar vortex that encircles Antarctica is less disturbed than its counterpart in the Northern Hemisphere because of the weaker stationary planetary wave perturbations forced by large-scale continental elevations and land-sea contrasts. Although the vortex may shift in position and deform in shape in response to wave perturbations, its integrity (as defined in ref. 15) is usually maintained until its breakdown in early November. It therefore appears that irreversible wave-induced transports¹⁶ do not effectively reach Antarctica during this period.

During the polar winter in the Southern Hemisphere, dynamical transport of heat into the circumpolar vortex is weak. Local temperatures in the Antarctic lower stratosphere have time to adjust so that cooling, $C(T)$, approximately balances diabatic heating, H , to reach low values¹⁷, approaching the radiative equilibrium temperature T_c (refs 18, 19), with $H - C(T_c) = 0$. The situation changes abruptly when the Sun returns. Absorption of solar radiation by O₃ causes H to increase rapidly as the number of sunlit hours increases. However, radiative cooling to space, which is temperature-sensitive, remains close to the low value achieved during the polar night. The temperature evolution is constrained by the prognostic zonal momentum and energy equations through the thermal wind relationship and mass continuity equation. Thus, local temperature can adjust only on a longer dynamical timescale, due to 'dynamical inertia'^{18,20}. In the absence of wave transports, the dynamical timescale is found²⁰ to be related to the newtonian cooling timescale of about 1-2 months for the Antarctic lower stratosphere²¹. The radiative imbalance temporarily leads to a positive net heating,

$$Q = H - C = \Delta H > 0 \quad (1)$$

where ΔH is the incremental increase in heating due to absorption of solar radiation.

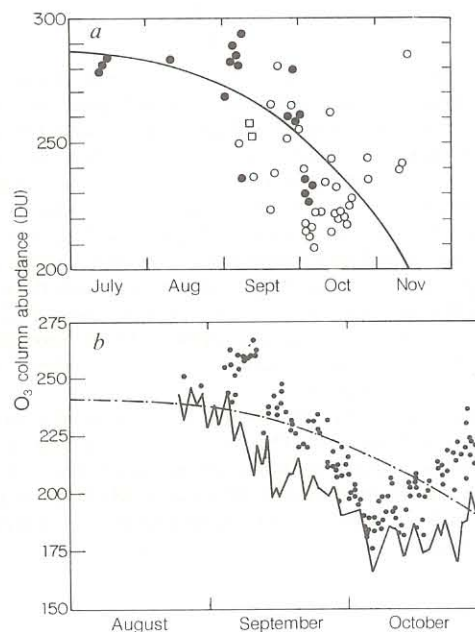


Fig. 2 *a*, Calculated column abundance (in Dobson units; 1 DU = 10⁻³ atm cm) of O₃ at 69° S (curve), compared with observations for the Syowa Station¹. The O₃ profile is calculated as described in Fig. 1 legend. The O₃ advected out of the top of the vortex (at ~30 km) is assumed to be swept away by horizontal motion and will not contribute to the column content. The data are from Dobson instrument by direct Sun (○), by cloudy zenith (□) and by Moon (●). *b*, Calculated column abundance of O₃ at 76° S (---) compared with observations from the Total Ozone Mapping Spectrometer (TOMS)³. The computation procedure is as stated in *a*, except that solar insolation is calculated for 76° S and the initial O₃ profile is adjusted to give an initial value of 240 DU for the column content. The data from TOMS³ comprise the minimum observed values for all longitudes between 74° S and 78° S (solid line) and observations at Halley Bay (dots).

The above increase in net heating may be balanced by an increase in local air temperature (T), or by a vertical ascent of the heated air mass or both. This follows from the zonal-mean thermodynamics equation, which is, neglecting wave transports,

$$\bar{Q} = \frac{\partial}{\partial t} \bar{T} + \Gamma \bar{w} \quad (2)$$

where $\Gamma = (\partial \bar{T} / \partial z) + 9.8 \text{ } ^\circ\text{C km}^{-1}$ is the static stability parameter, the overbar denotes the zonal mean and \bar{w} is the residual mean vertical velocity. Because of the 'dynamical inertia', the net heating should lead mainly to an upward circulation with vertical velocity

$$\bar{w} \approx \bar{Q} / \Gamma \quad (3)$$

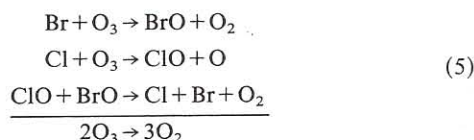
during early spring. The upward branch of this reverse circulation in the lower stratosphere occurs in the vortex where $\bar{T} < T_e$, while the downward branch occurs at the edge of the polar vortex where $\bar{T} > T_e$. As upwelling (subsidence) lowers (raises) the column density of O_3 , it follows from the above arguments that, during the Antarctic spring, cold (warm) temperature should be correlated with O_3 minimum (maximum) at the altitude where O_3 concentration is largest. This is consistent with observation³. In the northern polar stratosphere, winter temperatures are maintained by dynamical transport, leading to values $\sim 20\text{--}30 \text{ } ^\circ\text{C}$ warmer than the temperature that prevails over the southern winter pole. Radiative cooling thus tends to exceed heating in Arctic winter, resulting in a downward diabatic circulation, as evidenced by the movement of stratospheric aerosols²².

To estimate the effect of upwelling on O_3 , we use a simple model based on the zonal-mean equation for the O_3 mixing ratio \bar{f} ,

$$\frac{\partial \bar{f}}{\partial t} + \bar{v} \frac{\partial \bar{f}}{\partial y} + \bar{w} \frac{\partial \bar{f}}{\partial z} = 0 \quad (4)$$

where the effect of irreversible mixing and photochemical reactions are neglected. As the residual mean meridional velocity (\bar{v}) is small near the pole, the effect of horizontal transport is also neglected. Figure 1 shows the calculated heating rate, ΔH , due to the absorption of solar radiation by ozone alone. The vertical advective velocity is calculated using equations (3) and (1), as described in Fig. 1 legend. Figure 2a, b shows a comparison of our calculated column densities of O_3 with observations at Syowa Station for 1982 (ref. 1) and with those at the latitude of Halley Bay for 1983 (ref. 3). The calculated rate of decline in September and October appears to be consistent with the observed zonal mean values³, but is smaller than the minimum over all longitudes.

An assessment of the photochemical contribution is hampered by the lack of kinetic data. The following discussion should be viewed as an assessment of the requirements on photochemistry for it to explain the observed O_3 behaviour. McElroy *et al.*⁴ have proposed that catalysis of O_3 recombination involving the bromine-chlorine cycle²³ may be important in Antarctic early spring:



In order for reaction (5) to provide a decrease of 0.5% per day in the column abundance of O_3 , the 24-h-averaged abundances of ClO and BrO at $\sim 18 \text{ km}$ must be $\sim 0.4 \text{ p.p.b.v.}$ and 20 p.p.t.v. (parts per 10^{12} by volume), respectively.

Results of our two-dimensional model¹¹ indicate a total chlorine (ClY) mixing ratio of 2.6 p.p.b.v. in the upper stratosphere and 1.5 p.p.b.v. at 18 km, of which 30% is in the form of ClO_x ($\text{ClNO}_3 + \text{Cl} + \text{ClO} + \text{OCIO} + 2 \times \text{Cl}_2 + \text{HOCl}$). If the observed decrease in O_3 were to be explained by photochemistry alone, ClO would have to be the major ClO_x species in early

spring. The daytime abundances of the species Cl, ClO and ClNO_3 are primarily determined by the equilibrium between production of ClO by photolysis of ClNO_3 and rapid re-formation of ClNO_3 , with equilibrium achieved within 1–2 h of daylight²⁴. To maintain the high ClO concentration, we must consider processes which both convert ClNO_3 to ClO_y ($\text{Cl} + \text{ClO} + \text{OCIO} + 2 \times \text{Cl}_2 + \text{HOCl}$) and maintain sufficiently low NO_x to inhibit re-formation of ClNO_3 . It is also important to consider the initial conditions of chlorine and nitrogen species in late autumn when the polar vortex is established before entering polar night.

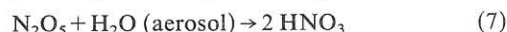
Figure 3 summarizes the possible chemical mechanisms controlling chlorine and nitrogen species from Antarctic late autumn to early spring. Net conversion of NO_x to N_2O_5 occurs in the late autumn due to the rapidly decreasing photolysis rates of N_2O_5 with increasing solar zenith angles and shorter days. As the NO_x decreases, the daytime ClO increases, until the ClO and NO_x concentrations are comparable. From that point on, all ClO and NO_x will be sequestered in ClNO_3 within 1–2 h of darkness. Under these conditions, we calculate daytime concentrations of ClO of 0.07 p.p.b.v. at 18 km during late autumn and early spring, corresponding to a 24-h-averaged ClO of 0.02 p.p.b.v.

Further net conversion of NO_x to N_2O_5 is possible only if there is another night-time sink for ClO to prevent formation of ClNO_3 . Bromine chemistry may provide such a mechanism through the reaction²⁵



The measured rate constant²⁵ implies a ClO time constant of 1 h for a BrO mixing ratio of 20 p.p.t.v. Conversion of ClO to OCIO by reaction (6) will dominate over ClNO_3 formation if the abundance of NO_x is $< 0.1 \text{ p.p.b.v.}$, again facilitating the conversion of NO_2 to N_2O_5 at night and correspondingly increasing the equilibrium concentration of ClO during the day by a factor of 3. Reaction (6) effectively removes all ClO at night, restricting the effect of reaction (5) to daytime only.

Photolysis of N_2O_5 would constitute an important source of NO_x within 1 week after emergence from polar night, thus re-forming ClNO_3 at the expense of ClO. Concentrations of N_2O_5 may be kept low by assuming the heterogeneous reaction²⁶



with an equivalent first-order rate of 10^{-6} s^{-1} near 18 km. This rate implies values of 10^{-2} for γ , the probability of reaction per collision with an aerosol surface, if we assume the background

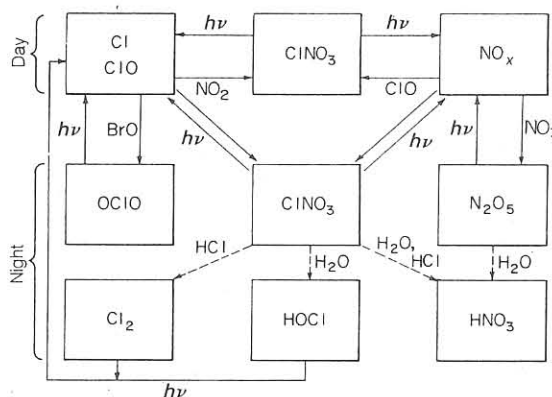
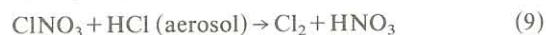


Fig. 3 Schematic diagram of the possible chemical mechanisms controlling nitrogen and chlorine species from late autumn to early spring in Antarctica. Species in the upper ('day') and lower ('night') portions are formed primarily during the day and night, respectively. Dashed lines; reactions proceeding through both homo- and heterogeneous channels. We note that although HOCl and HNO_3 are produced primarily during the day for mid-latitude conditions, such production is negligible for high-latitude late autumn to early spring, due to the low abundances of OH and HO_2 .

aerosol concentrations of ref. 27. The required value of γ could be reduced by more than a factor of 10 if we adopt the enhanced aerosol abundances for periods of high volcanic activity or the existence of polar stratospheric clouds²⁸.

Other heterogeneous processes have been proposed to convert ClNO₃ to ClO_y and maintain low NO_x concentration. We find that the reactions^{4,5,32}



could achieve substantial conversion of ClNO₃ if an equivalent first-order rate of 10⁻⁶ s⁻¹ is assumed, leading to daytime ClO abundances in August of 0.5 p.p.b.v. and 1 p.p.b.v. with reactions (8) and (9), respectively. Higher rates are needed if reactions (8) and (9) are to counteract the production of NO_x by photolysis of HNO₃ a month after emergence from polar night⁴. In our proposed model upwelling may become important at this time, lowering the concentrations of ClY as well as O₃, and reducing the importance of photochemistry. The extent of photochemical depletion during the first month will, however help determine the magnitude of the subsequent October minimum and possibly contribute to the interannual trend.

The above discussion pertains to seasonal variations of Antarctic ozone and does not address the observed interannual trend of decreasing October minimum values since 1979 (refs 2, 3) While theories based on chemistry mostly attribute the secular trend to increases in stratospheric chlorine^{2,4,5}, enhanced upwelling over recent years may also play a part. Aerosol loading of the Antarctic stratosphere has increased by almost an order of magnitude in recent years²⁹, due probably to a series of major volcanic eruptions since 1979. Absorption of solar radiation by aerosol particles³⁰ would increase ΔH . During the polar night, increased cooling in the 10–50 mbar region from the higher aerosol loading could lead to a more negative vertical temperature gradient and a smaller Γ . Equation (3) then implies a stronger upwelling when the Sun returns. Our present calculation does not incorporate these additional factors and presents only a baseline model for a 'clean' atmosphere, designed to demonstrate the seasonal trend.

The proposed mechanisms (dynamical and chemical) have

different implications for the susceptibility of stratospheric O₃ to atmospheric perturbations, and may manifest themselves in different ways and at different times in spring. The chemical mechanism may be dominant during the initial decline after the return of the Sun, when the strength of upwelling is still weak. Thereafter, however, the ClY concentrations may be reduced by the upwelling, effectively diminishing the catalytic removal of O₃. Future measurements should be aimed at evaluating the relative importance of the two separate processes.

The radiative-dynamical mechanism we have described should be reflected in the temporal and spatial behaviour of many long-lived species and stratospheric aerosol. As a result of the existence of the reverse circulation, we may expect to see increasing abundances of 'upward-diffusing' species (such as chloro-fluorocarbons, N₂O and CH₄) and decreasing concentrations of 'downward-diffusing' species (HNO₃, HCl, stratospheric aerosol) during early spring in the Antarctic lower stratosphere. Simultaneous observations of these trace gases and aerosols will be useful. Observations of the vertical temperature gradient will determine values for Γ , providing better estimates of \bar{w} from ΔH .

The chemical mechanisms require concentrations of ~0.5–1 p.p.b.v. for ClO and 20 p.p.t.v. for BrO. Levels of OClO comparable to those of daytime ClO could be obtained at night starting in late autumn, if sufficient BrO is present. The OClO is photolysed within minutes after sunrise, with a correspondingly rapid increase in ClO. Observations of the diurnal variation of both ClO and OClO will yield indirect evidence of the magnitude of the BrO abundance. Measurements of NO₂ in the lower stratosphere are also needed. The technology for measuring these species is presently available and should be used.

This research has been supported by NASA grants NAGW-798 to MIT and NAGW-4080 to AER. K.-K.T. acknowledges support from the John Simon Guggenheim Foundation during his sabbatical year. Work at AER is also supported by the Fluorocarbon Program Panel of the Chemical Manufacturers Association. We thank M. McIntyre, M. Prather and A. Tuck for comments, S. Chubachi for reprints, and M. McElroy, S. Solomon and R. Stolarski for providing us with their results before publication.

Received 7 March; accepted 12 June 1986.

- Chubachi, S. in *Proc. Quadrenn. Ozone Symp.* (eds Zerefos, C. S. & Ghazi, A.) (Reidel, Dordrecht, 1985).
- Farman, J. C., Gardina, B. G. & Shanklin, J. D. *Nature* **315**, 207–210 (1985).
- Stolarski, R. S. *et al. Nature* **322**, 808 (1986).
- McElroy, M. B., Salawitch, R. J., Wofsy, S. C. & Logan, J. A. *Nature* **321**, 759–761 (1986).
- Solomon, S., Garcia, R. R., Rowland, F. S. & Wuebbles, D. J. *Nature* **321**, 755–758 (1986).
- Brewer, A. W. *Q. Jl R. met. Soc.* **75**, 351–363 (1949).
- Dobson, G. M. B. *Proc. R. Soc. A235*, 187–192 (1956).
- Murgatroyd, R. J. & Singleton, F. Q. *Jl R. met. Soc.* **87**, 125–135 (1961).
- Dunkerton, T. *J. Atmos. Sci.* **35**, 2325–2333 (1978).
- Tung, K. K. *J. Atmos. Sci.* **39**, 2230–2355 (1982).
- Ko, M. K. W., Tung, K. K., Weisenstein, D. K. & Sze, N. D. *J. geophys. Res.* **90**, 2313–2329 (1985).
- Solomon, S., Garcia, R. R. & Stordal, F. *J. geophys. Res.* **90**, 12981–12990 (1985).
- Dütsch, H. U. *Pure appl. Geophys.* **116**, 511–529 (1978).
- Bowman, K. P. & Krueger, A. J. *J. geophys. Res.* **90**, 7967–7976 (1985).
- McIntyre, M. E. *J. met. Soc. Japan* **60**, 37–65 (1982).
- McIntyre, M. E. & Palmer, T. N. *Nature* **320**, 593 (1983).
- Murgatroyd, R. J. in *The Global Circulation of the Atmosphere* (ed. Corky, G. A.) (Royal Meteorological Society, London, 1969).

- Fels, S. B., Mahlman, J. D., Schwarzkopf, M. D. & Sinclair, R. W. *J. Atmos. Sci.* **37**, 2265–2297 (1980).
- Wehrbein, W. M. & Leovy, C. B. *J. Atmos. Sci.* **39**, 1532–1544 (1982).
- WMO/NASA, *Atmospheric Ozone: Assessment of our Understanding of the Process Controlling its Present Distribution and Changes* (in the press).
- Kiehl, J. T. & Solomon, S. *J. Atmos. Sci.* (in the press).
- Kent, G. S., Trepte, C. R., Farrukh, U. O. & McCormick, M. P. *J. Atmos. Sci.* **42**, 1536–1551 (1985).
- Yung, Y. L., Pinto, J. P., Watson, R. T. & Sanders, S. P. *J. Atmos. Sci.* **37**, 339–353 (1980).
- Ko, M. K. W. & Sze, N. D. *J. geophys. Res.* **89**, 11619–11632 (1984).
- Clyne, M. A. A. & Watson, R. T. *JCS Faraday Trans. 1*, **73**, 1169 (1977).
- Wofsy, S. C. *J. geophys. Res.* **83**, 364–378 (1978).
- Turco, R., Hamill, P., Toon, O. B., Whitten, R. C. & Kiang, S. S. *J. Atmos. Sci.* **36**, 699 (1979).
- McCormick, M. P., Steele, H. M., Hamill, P., Chu, W. P. & Swisler, T. J. *J. Atmos. Sci.* **39**, 1387–1397 (1982).
- Hoffman, D. J. & Rosen, J. M. *Geophys. Res. Lett.* **12**, 13–16 (1985).
- Mugnai, A., Fiocco, G. & Grams, G. Q. *Jl R. met. Soc.* **104**, 783–796 (1978).
- Strobel, D. F. *J. geophys. Res.* **83**, 6225–6230 (1978).
- Rowland, F. S., Sato, H., Ichwaja, H., Elliott, S. M. *J. Phys. Chem.* **90**, 1985–1988 (1986).